Durable infrared optical coatings based on pulsed DC-sputtering of hydrogenated amorphous carbon (a-C:H)

DES GIBSON[1], SHIGENG SONG[1*], LEWIS FLEMING[1], SAM AHMADZADEH[1], HIN ON CHU[1], STEPHEN SPROULES[2], RYAN SWINDELL[3], XIAOLING ZHANG[4], PARNIA NAVABPOUR[4], CASPAR CLARK[5], MARK BAILEY[5]

[1]Institute of Thin Films, Sensors and Imaging, Scottish Universities Physics Alliance
School of Computing, Engineering and Physical Sciences, University of the West of Scotland, Paisley PA12BE, UK
[2] WestCHEM, School of Chemistry, University of Glasgow, Glasgow G12 8QQ, UK
[3]Qioptiq Ltd, Glascoed Road, St Asaph LL17 0LL, Denbighshire UK
[4]Teer Coatings Ltd, West Stone House, West Stone, Berry Hill Industrial Estate, Droitwich, Worcestershire, WR9 9AS, UK
[5]Helia Photonics Ltd, Rosebank Park, Livingston West Lothian EH54 7EJ, Scotland, UK

**Corresponding author: shigeng.song@uws.ac.uk*

Abstract: Optical, mechanical, stress and environmental properties of room temperature pulsed DC sputter deposited hydrogenated carbon are presented. Increasing hydrogen incorporation into the sputter deposited carbon significant decreases infrared optical broadband. Mechanism for reduced absorption is due to a decrease in deep absorptive states associated with dangling bonds. Hydrogen flow is optimized to achieve best compromise between increased infrared spectral transmittance and hardness to achieve durable infrared anti-reflection coatings. Optical, environmental and durability performance indicates suitability as a durable infrared optical coating for commonly used infrared substrates such as germanium, zinc sulfide, zinc selenide and chalcogenide glass.

OCIS CODES: (310.1860) Deposition and fabrication; (310.3840) Materials and process characterization; (310.1860) Thin films, optical properties

1. INTRODUCTION

Attention has been focused in recent years on the need for robust protective anti-reflection coatings for infrared (IR) optical materials used in applications requiring use in severe environments such as autonomous vehicle imaging systems (Ref. [1]). Current IR window materials such as forward looking infrared (FLIR) zinc sulfide (ZnS), germanium (Ge) and moldable chalcogenide glasses exhibit acceptable optical performance. However, these materials have inadequate performance in relation to mechanical and environmental properties (Ref. [2]) with the problem illustrated in Figure 1a.

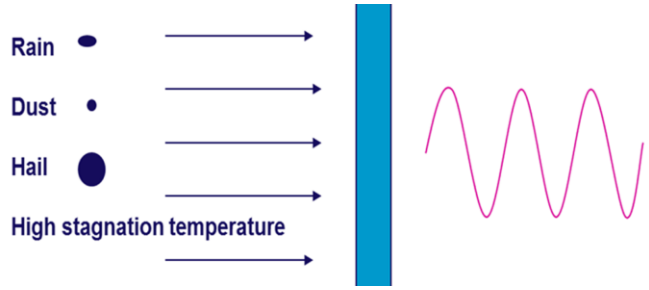

Fig 1a. Problem – Use and protection of soft/brittle infrared materials in harsh environments.

The use of hard, high-Youngs modulus transparent coatings is one of the most important methods of protecting optical components (Ref. [2]), with the solution shown in Figure 1b.

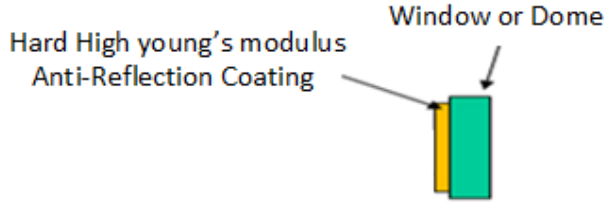

Fig 1b. Solution – Hard, high Young's-modulus transparent Anti-Reflection coatings.

Various coatings have been investigated for protecting FLIR ZnS and Ge based on radio-frequency plasma enhanced chemical vapour deposition (PECVD) of amorphous hydrogenated carbon (a-C:H, also referred to as diamond-like-carbon (DLC)) (Ref. [3, 4]), germanium carbide (GeC Ref. [5]) and boron phosphide (BP Ref. [6]). However, PECVD methods have limited throughput and typically require high substrate temperature during deposition (DLC 120°C (Ref. [3, 4]); GeC (Ref. [5]) and BP (Ref. [6]) typically 300°C), precluding use for high throughput applications (Ref. [1])

and use for temperature sensitive substrates like moldable chalcogenide glass (Ref. [7]).

Previous amorphous hydrogenated carbon coatings have been achieved through radio-frequency magnetron sputtering (Ref. [8, 9]) and DC sputtering (Ref. [10, 11, 12]), using hydrocarbon feedstock to modify deposited film visible optical transmittance, stress and material structural properties.

This paper describes performance of room temperature pulsed-DC sputtering of hydrogenated amorphous carbon (a-C:H) infrared optical coatings based on a high throughput drum configuration (Ref. [13]). Use of the beneficial influence of hydrogenation during the deposition process is described, achieved through the controlled introduction of hydrogen during pulsed DC sputter deposition. Hydrogenation passivates the free electron dangling bonds, reducing their concentration from typically 10^{19} to 10^{16} cm^{-3} (Ref. [14]), leading to a significant reduction in infrared optical absorption.

Novelty in this work is use of hydrogenation during pulsed-DC sputtering of carbon to reduce infrared optical absorption to a level required for use as an infrared optical coating. As hydrogenation reduces the deposited carbon film density and hardness, this work identifies optimal hydrogenation conditions for reduced infrared absorption and providing sufficiently hard and high Youngs modulus coating performance.

2. EXPERIMENTAL

A. DEPOSITION SYSTEM AND PARAMETERS

Deposition was carried out using a pulsed DC reactive sputtering process with microwave plasma for chamber pre-conditioning to reduce vacuum water content and substrate pre-cleaning. Schematic of the drum based deposition system configuration is shown in Figure 2.

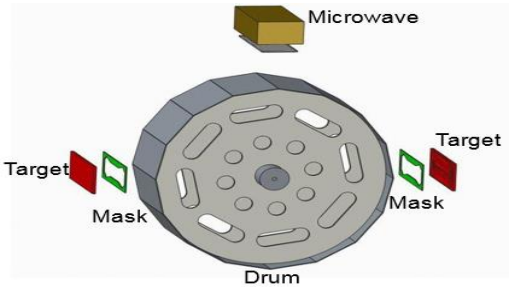

Fig 2. Schematic of Microwave Assisted Pulsed DC Sputter System.

Vacuum pumping to a final system base pressure of $5E^{-7}$ mbar is achieved using a combination of turbo (Osaka Vacuum 1500L/s) and cryocooler water vapor pumping (IGG polycold).

Deposition conditions are provided in the following table 1 for deposited hydrogenated carbon (low refractive index material) and germanium (high refractive index material). All sputter deposition carried out with no direct substrate heating. Temperature was monitored by thermocouples within the chamber. Peak temperature reached during sputter deposition was ≤70°C (heating due to sputter deposition process).

Deposition conditions provided in following table 1 for pulsed DC sputter deposited hydrogenated carbon (low refractive index material) and germanium (high refractive index material), providing deposition capability for a-C:H/ germanium multilayers.

Table 1. Typical deposition conditions pulsed DC sputtered hydrogenated carbon and germanium.

Parameter	Amorphous Carbon	Polycrystalline Germanium
Ar Flow (sccm)	100	190
H_2 Flow (sccm)	0 to 18	3
Gas purities (%)	99.99	99.99
Process Pressure (mTorr)	4	3.7
Base Pressure (mBar)	$5x10^{-7}$	
Power (kW)	4	2.5
Current (A)	10	5.92
Voltage (V)	400	423
Pulse Conditions		
Pulsed DC Frequency (kHz)	46	75
Pulse Duration (µs)	4	13
Reverse Pulse (as percentage of forward pulse voltage) (%)	20	20
Deposition rate (Å/s)	0.3	1.1
Target purity (%)	99.99	99.99
Preclean microwave plasma power (kW)	3*	
Chamber pre-conditioning & Substrate Preclean Time (Mins)	30	
Thickness (nm)	200 to 1200	200 to 700
Comment	* No microwave used during deposition.	

The deposition system used an electrically floating horizontal axis rotating drum (anode is the grounded chamber with no external bias applied to the drum). Deposition of each layer can be achieved with multiple passes across a rectangular planar magnetron source. Reverse pulse (+ve cycle) was 20% of the forward (-ve) pulse voltage for both carbon and polycrystalline Germanium. Pulsing conditions optimized to reduce sputter target arcing.

B. CHARACTERISATION AND DATA ANALYSIS

Infrared substrates coated were germanium, zinc sulfide, zinc selenide, gallium arsenide, chalcogenide (Schott IG4 (Ref. [15]). Characterization methods and associated data analysis described as follows.

1. *SPECTRAL TRANSMITTANCE & OPTICAL CONSTANT EVALUATION*

Spectral transmittance was measured using a Nicolet iS50 Fourier transform Infrared Spectrophotometer as a function of hydrogen flow for all coated substrates.

Minimum-to-maximum transmission difference is an indicator of refractive index (increased minimum-to-maximum transmission indicates increasing refractive index). Refracve index (n(λ)) and extinction coefficient (k(λ)) dispersion characteristics are derived from the measured spectral transmittance characteristics using the Stephen K. O'Leary, S. R. Johnson, and P. K. Lim (OJL) model (Ref. [16]) and the Kramers–Kronig relationship (Ref. [17,18]).

Optical performance described in section 3.

2. *HARDNESS AND YOUNGS MODULUS MEASUREMENT*

The hardness and Young's modulus of the coatings were determined using a Fischerscope H100 tester, with a Vickers' indenter from the load penetration curves (Ref. [21]). Five indents were made on each sample and the data averaged. The maximum indentation load applied was 50 mN and the loading unloading rate was 10 mNs^{-1}.

A typical load and unload curve for a pulsed DC sputtered a-C:H film is shown in Figure 3. Extrapolation of data slope (S in Figure 3) and use within method described in Ref [21], are analyzed within the equipment software automatically to extract hardness and Youngs modulus data. Ref. [22].

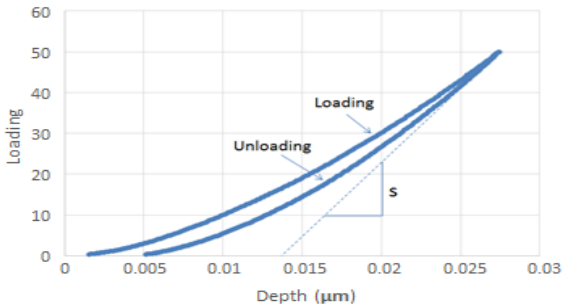

Fig. 3, Load and unload curve for a typical pulsed DC sputtered hydrogenated amorphous carbon film.

Hardness and Youngs modulus performance described in section 4A.

3. *AVERAGE STRESS MEASURMENT AND CALCULATION*

The average film stress is calculated from the change in curvature of an elastically deformed coated substrate (100mm diameter, 300um thick silicon wafer). Stress is calculated using the Stoney formula Ref. [23].

An E+H Metrology, GmbH (model MX- 203-6-33) gauge using capacitive distance sensors, was used to measure wafer geometry before and after coating deposition. The equipment automatically calculates the coating stress based on the Stoney formula [23]. Stress performance described in section 4B.

4. *ENVIROMENTAL AND DURABILITY TESTS*

Environmental/durability tests were performed on all coated substrates based on the following MIL-C-48497A test Ref [24] relevant to external surface optical coatings – specific ML-C-48497A tests summarised in table 2.

Table 2: Details of environmental/durability tests.

Test	Specification	Description
Adhesion	MIL-C-48497A Section 4.5.3.1	Press adhesive cellophane tape firmly against the coated surface and quickly remove at an angle normal to the coated surface
Severe Abrasion	MIL-C-675C Section 4.5.10	40 strokes with rubber eraser loaded at 1kg
Humidity	MIL-C-48497A Section 4.5.3.2	24 hours at 49°C and humidity greater than 95%
Temperature	N/A	16 hours at +95°C, 16 hours at -54°C
Salt water solubility	MIL-C-48497A Section 3.4.3.2	24 hour immersion in salt water solution

Environmental/durability results described in section 6.

3. OPTICAL PERFORMANCE

A. INFRARED SPECTRAL TRANSMITTANCE

Infrared spectral transmittance is shown in Figure 4

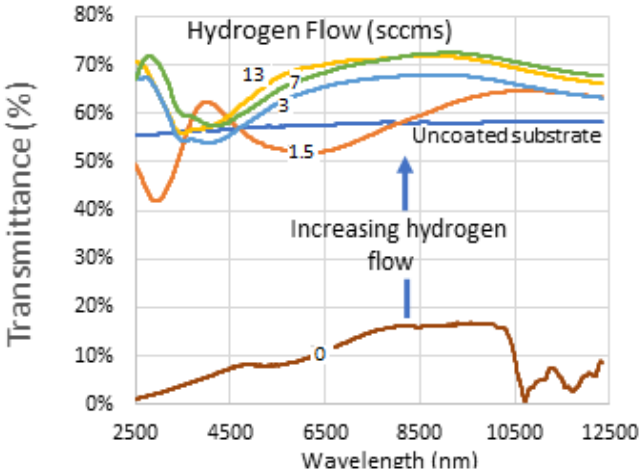

Fig 4. Influence of hydrogen flow on infrared spectral transmittance spectra for single layer (typically 1 µm thickness) sputtered pulsed DC a-C-H thin films deposited onto GaAs substrates.

Figure 4, demonstrates effectiveness of hydrogenation during a-C:H deposition, providing increased infrared transmittance (reduced absorption) with increasing hydrogen flow.

B. OPTICAL CONSTANTS

Figures 5a and b show a-C:H infrared refractive index (n(λ)) and extinction coefficient (k(λ)) dispersion characteristics respectively as a function of hydrogen flow during deposition. n(λ) and k(λ) dispersion data shown in Figures 5a and b respectively - derived from measured spectral photometric data using Stephen K. O'Leary, S. R. Johnson, and P. K. Lim (OJL) model (Ref. [16]) and the Kramers–Kronig relationship (Ref. [17,18]).

PECVD a-C:H n/ k at wavelength 10um and 12um are typically 2.00/ 2.00.10^{-2} and 2.00/4.5.10^{-2} respectively (Ref. [4, 19]), indicating pulsed DC sputtered films have optical properties suited to use in the infrared.

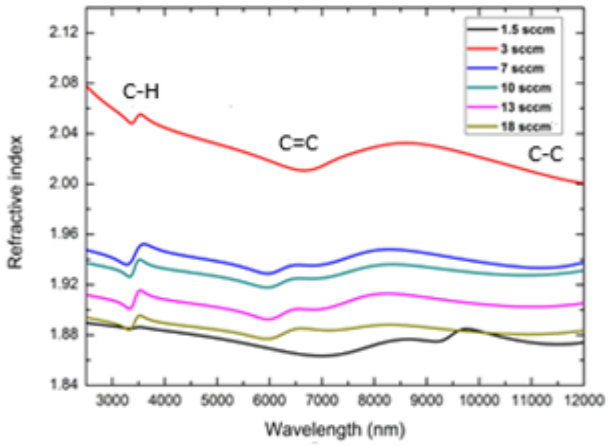

Fig 5a. Pulsed DC sputtered hydrogenated carbon refractive index for hydrogen flow rates of 1.5, 3, 7, 10, 13 and 18 sccm (C-H, C-C, C=C absorption bond spectral regions indicated).

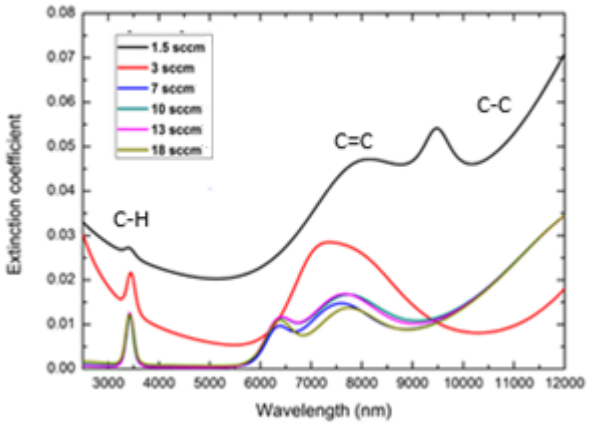

Fig 5b. Extinction coefficient vs. infrared wavelength for hydrogen flow rates of 1.5, 3, 7, 10, 13 and 18 sccm (C-H, C=C, C-C absorption bond regions indicated).

From Figure 5b, it can be seen that C-H, C=C and C-C bond stretching is observed by peaks found in the extinction coefficient data. C-H bond stretching is assigned for wavelengths around 3.43 µm, 6.00-6.50 µm is associated with C=C bond stretching. A trend observed is increasing hydrogen flow lowers the extinction coefficient due to a decrease in deep absorptive states associated with free electron dangling bonds (Ref. [14]).

It is likely that the increased hydrogen content reacts with the π-bonds, leading to hydrogenation in the amorphous carbon films (Ref. [14]). This would reduce the carbon-carbon double bond content, implying less states would contribute to the C=C bond stretch observed in Figure 4b. These mid-IR absorptions can be interpreted as electronic transitions between localized π and π* states. (Ref. [19]). A tail from C-C bond absorption at higher wavelengths is observed for all samples, although this absorption is part of the fingerprint region of the IR spectra. This assignment of sp^3 C-C bond stretching is for the tail from the 7.6 µm – 12.5 µm region. (Ref. [20])

Figures 6a and b show variation in n and k respectively with increasing hydrogen flow at wavelengths 3, 5, 9 and 11 µm.

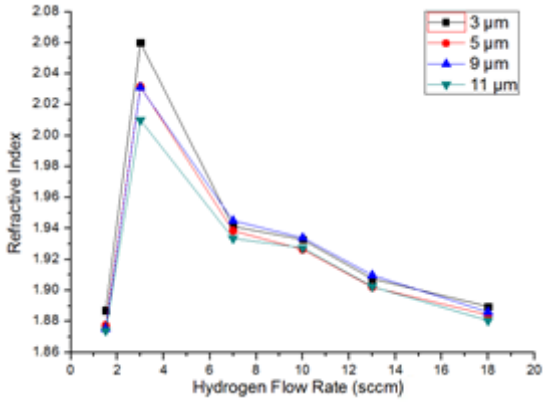

Fig 6a. Refractive index vs. Hydrogen flowrate for infrared wavelengths 3, 5, 9 and 11 µm.

Reducing refractive index with increasing hydrogen flow is a consequence of decreasing film density.

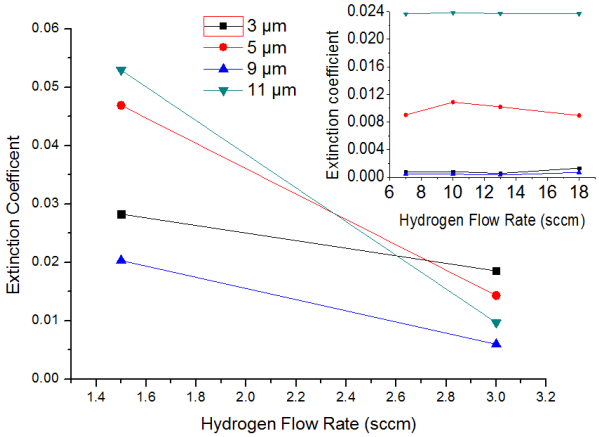

Fig 6b. Extinction coefficient vs. Hydrogen flowrate for various infrared wavelengths (3, 5, 9 and 11 µm) – shown separately for low (≤3sccms) and high (≥7sccms) hydrogen flows.

Future work is planned to investigate the mechanisms underlying the spectral characteristics shown in Figures 6a and b.

Extinction coefficient for deposited carbon with no hydrogen introduction is typically 0.6 (not shown in Fig 6b). Introduction of hydrogen flow ≥3sccms during deposition leads to a reduction in extinction coefficient by typically a factor of 20.

C. C-H CONTENT WITH INCREASING HYDROGEN

Figures 7 presents estimated relative C-H bond content (based on extinction coefficient area at C-H bond stretching absorption wavelength 3.43 µm) with increasing hydrogen flow.

A Gaussian/Lorentzian peak fitting was applied to the extinction coefficient peak at 3.43 µm and peak area was derived and subsequently normalized with respect to the 1.5 sccm a-C:H data for comparison.

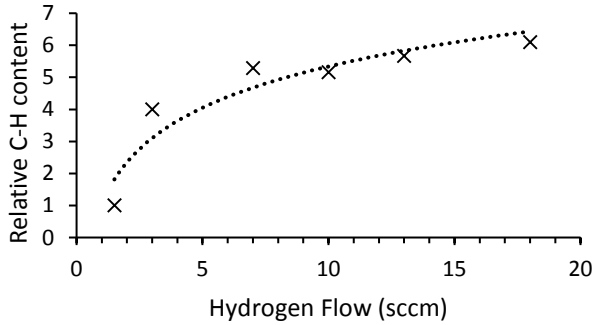

Fig 7. Extinction coefficient at 3.43µm against hydrogen flow. Estimated C-H content, based on peak areas from the extinction coefficient vs wavelength data, relative to 1.5 sccm a-C:H.

Results indicate minimal increase in incorporated hydrogen for hydrogen flows ≥7sccms.

4. HARDNESS & YOUNGS MODULUS AND STRESS PERFORMANCE

A. HARDNESS & YOUNGS MODULUS

Results are shown in Figures 8a and b, indicating Vickers hardness and Youngs modulus respectively. Hardness ranges from 1000 to 2400 kg/mm^2 for pulsed DC sputtered a-C:H with increasing hydrogen flow. Typical PECVD DLC Vickers hardness level is 1500 to 2000 kg/mm^2 (Ref. [22]).

Hardness reduces with increasing hydrogen flow due to decreasing film density. Hardness and Youngs modulus trend shows minimal change for hydrogen flow ≥7sccms, in line with results shown in figures 8a and b, indicating minimal increase in incorporated hydrogen for hydrogen flow ≥7sccms.

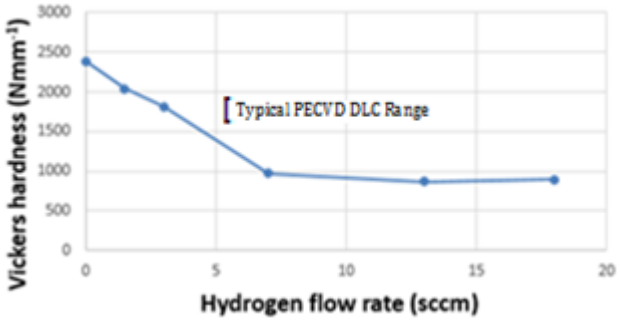

Figure 8a, Pulsed DC sputtered a-C:H Vickers hardness with increasing hydrogen flow. Typical PECVD a-C:H hardness range is shown (Ref, [22]).

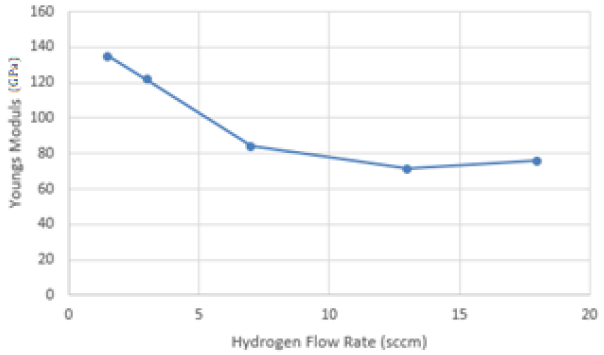

Figure 8b, Pulsed DC sputtered a-C:H Youngs modulus (GPa) with increasing hydrogen flow. Typical PECVD a-C:H Young`s modulus range is 120 to 140Gpa [22]

B. STRESS PROPERTIES

Results are shown in Figure 9, indicating pulsed DC sputtered hydrogenated amorphous carbon film stress with increasing hydrogen flow. Stress is compressive and reduces with increasing hydrogen flow

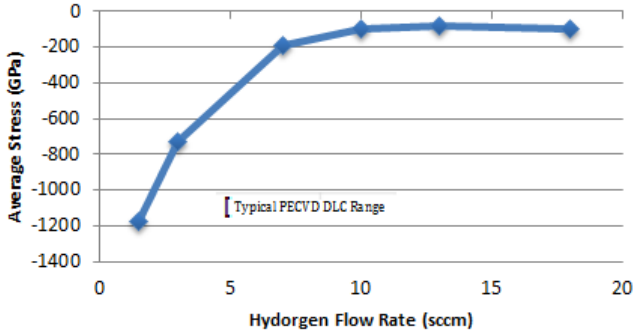

Figure 9 Pulsed DC sputtered a-C:H stress with increasing hydrogen flow. Typical PECVD a-C:H stress range shown (Ref. [22])

Stress is compressive and reduces with increasing hydrogen flow, with minimal change for hydrogen flow ≥7sccms, in line with results shown in figure 6. Typical PECVD a-C:H stress level is 1000 to 1200 kg/mm^2 (Ref. [22]).

5. 8 TO 12µm a-C:H/Ge MULTLAYER ANTI-REFLECTION COATING AND OPTICAL PERFORMANCE

Based on optical and hardness evaluation of the pulsed DC sputtered a-C:H (low refractive index film), described in sections 3 and 4 respectively, best compromise between increased infrared spectral transmittance, reduced stress and maximised hardness/ Youngs modulus is achieved with 3sccm hydrogen flow during pulsed DC sputter deposition.

Germanium (high index material) was sputtered using the same conditions indicated in Table 2, utilising a hydrogen flow of 3sccms. Pulsed DC sputtered Ge refractive index and extinction coefficient are typically 4 and 0.0005 respectively, over the 8 to 12um with no significant change in refractive index and extinction coefficient for hydrogen flow greater than 3sccms. As such absorptive loss within the anti-reflective coating is dominated by the a-C:H film.

An a-C:H (low refractive index)/ Ge (high refractive index) 8 o 12um anti-reflective multilayer was designed using a-C:H refractive index/ extinction coefficient dispersion data provided in section 3B and germanium index and extinction coefficient of 4 and 0.0005 respectively.

A four layer coating was designed using thin film design software Essential Macleod, (Ref. [25]). The design was optimised for maximum optical transmittance and minimum reflectance over the 8 -12 and 8-14 micron spectral ranges. Design optimisation required a minimum of four layers (no significant optical benefit achieved with greater than four layers).

The design includes alternating germanium carbon layers with respective physical thicknesses shown in table 3 (typical deposition time is fourteen hours based on deposition rates shown in Table 1):

Table 3: Four layer design layer thicknesses

Layer number (from substrate)	Material	Physical Thickness (nm)
1	Germanium	262
2	Carbon	229
3	Germanium	649
4	Carbon	1155

Design optimiisation was constrained to place the harder and high Youngs modulus a-C:H film at the outer surface of the four layer anti-reflection coating, thereby maximizing external surface durability. Design and measured averaged transmittance (T) and reflectance (R) over spectral ranges 8-12um and 8-14um are provided in the following Table 4 (substrate chalcogenide glass (Ref [15]).

Table 4: Design and measured averaged transmittance T and reflectance R over spectral ranges 8-12 µm and 8-14 µm (1mm thick substrate with high efficiency anti-reflection coating on reverse face)

	Wavelength Range (µm)			
	8-12		8-14	
	Design	Measured	Design	Measured
Transmittance	92.8%	91%	87%	85%
Reflectance	1.1%	1.3%	2.8%	3.5%

Typical PECVD a-C:H average transmittance (8 to 12 µm) is 89% (1mm thick Ge substrate with high efficiency anti-reflection coating on reverse face) - lower average transmittance due to both higher 8 to 12 µm extinction coefficient and also single later a-C:H anti-reflection coating (with PECVD difficult to achieve multilayer a-C:H/ Ge multilayers due to lack of precursors for PECVD germanium deposition, hence single layer a-C:H data quoted Ref [3,4]).

Spectral optical absorptance (1-T-R with substrate absorption deconvoluted) of the four layer pulsed DC hydrogenated sputter deposited C/Ge anti-reflective multilayer coating is shown in Figure 10. This shows the prominence of C=C and C-C absorption states, increasing average absorptance over the 8 to 12 µm waveband by typically 2%.

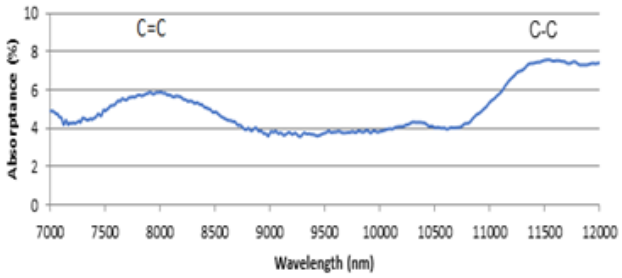

Figure 10, Four layer a-C:H/ Ge anti-reflection multilayer spectral absorptance (substrate absorption deconvoluted)

6. 8 TO 12µm a-C:H/Ge MULTLAYER ANTI-REFLECTION COATING ENVIRONMENTAL & DURABILITY PERFORMANCE

The four layer 8 TO 12µm a-C:H/Ge multilayer anti-reflection coatings on germanium, zinc sulfide, zinc selenide and chalcogenide substrates (Ref. [15]) pass all external surface coating tests defined in Table 2.

The tests outlined in Table 2 Ref [24] were selected based on typical requirements for IR optical coatings for use in harsh environments. The 8 to 12 coated samples passed the environmental tests and match performance of PECVD a-C:H Ref [4,19].

7. SUMMARY AND CONCLUSIONS

In this work room temperature pulsed DC sputtering of a-C:H is described. Increasing hydrogen incorporation into the sputter deposited a-C:H significantly decreases infrared broadband optical absorption. Mechanism for reduced absorption is a decrease in deep absorptive states associated with free electron dangling bonds (Ref. [8]).

Increasing hydrogen incorporation reduces deposited film density with a consequent reduction in hardness, Youngs modulus and compressive stress. As such hydrogen flow is optimized to achieve best compromise between increased infrared spectral transmittance, maximized refractive index, minimal extinction coefficient and high hardness & Youngs modulus to achieve durable infrared anti-reflection coatings. Optimal hydrogen flow during pulsed DC deposition was assessed as 3sccms.

Comparison of infrared optical, hardness, Youngs modulus and stress properties of pulsed DC sputtered a-C:H using 3sccms hydrogen flow during deposition and PECVD a-C:H (Ref.[4,19]) is provided in the following Table 5.

Table 5: Comparison of optical, hardness, Youngs modulus and stress properties of pulsed DC sputtered hydrogenated carbon (@ hydrogen flow 3sccms) and PECVD a-C:H (Ref.[4,19])

	Pulsed DC sputtered a-C:H (hydrogen flow 3sccms)	PECVD a-C:H (Ref, [2, 3, 11, 22])
n @ 10um	2.03	2.05
k @ 10um	0.01	0.02
Vickers Hardness kg/mm^2	1800	1800
Young's modulus GPa	130	150
Stress MPa (compressive)	-700	-1100

Optical, environmental and durability performance indicate suitability as a durable infrared optical coating for commonly used infrared substrates such as germanium, zinc sulfide, zinc selenide and chalcogenide glass, matching performance of PECVD a-C:H (Ref. [4,19]).

This paper demonstrates a novel pulsed DC drum based a-C:H sputtering process compared to PECVD a-C:H. The sputtering process provides a number of key advantages – low temperature operation (hence compatible with deposition onto temperature sensitive substrates such as chalcogenide glass), high throughput based on rotating drum format and provision of multilayer anti-reflection optical coating processes which provide increased transmittance/ reduced reflectance over extended spectral ranges.

Funding Information.
This work was funded by InnovateUK Manufacturing & Materials Round 2, Project No.103752.

Acknowledgment.
Input from the following s acknowledged - Hugh Frizell, Dr. Liz Porteous, Gerry O'Hare, and Jim Orr for their input to this project. Also ongoing support from the Scottish Universities Physics Alliance (SUPA).

Conflict of interest
The authors confirm there is no conflict of interest.

8. REFERENCES

1. J. Kim, S. Hong, J. Baek, E. Kim, and H. Lee, "Autonomous vehicle detection system using visible and infrared camera," in 2012 12th International Conference on Control, Automation and Systems (2012), pp. 630–634.
2. D. C. Harris and Society of Photo-optical Instrumentation Engineers., Materials for Infrared Windows and Domes: Properties and Performance (SPIE, 1999).
3. A. H. Lettington, "Optical properties and applications of diamond and diamondlike carbon thin films," in C.-G. Ribbing, ed. (International Society for Optics and Photonics, 1990), Vol. 1275, p. 14.
4. X. Fu, L. Li, G. Des, W. Ewan, and W. Lv, "Modelling and optimization of film thickness variation for plasma enhanced chemical vapour deposition processes," Chinese Opt. Lett. 11, S10209 (2013).
5. L. A.H., L. J.C., C. Wort, M. B.C., and A. Hope, "Developments in GeC as a durable IR Coating Material," E-MRS Meet. **17**, 469–474 (1987).
6. D. R. Gibson, E. M. Waddell, S. A. D. Wilson, and K. L. Lewis, "Ultradurable phosphide-based antireflection coatings for sand and rain erosion protection," Opt. Eng. 33, 957 (1994).
7. J. Huddleston, J. Novak, W. V Moreshead, A. Symmons, and E. Foote, "Investigation of As40Se60 chalcogenide glass in precision glass molding for high-volume thermal imaging lenses," in Proc.SPIE (2015), Vol. 9451.
8. C. R. Lin, D. H. Wei, C. K. Chang, and W. H. Liao, "Optical properties of Diamond-like Carbon films for antireflection

coating by RF magnetron sputtering method," in Physics Procedia (Elsevier B.V., 2011), Vol. 18, pp. 46–50.
9. R. Kleber, M. Weiler, A. Krüger, S. Sattel, G. Kunz, K. Jung, and H. Ehrhardt, "Influence of ion energy and flux composition on the properties of plasma-deposited amorphous carbon and amorphous hydrogenated carbon films," Diam. Relat. Mater. 2, 246–250 (1993).
10. L. Marcinauskas, V. Dovydaitis, A. Iljinas, and M. Andrulevičius, "Structural and optical properties of doped amorphous carbon films deposited by magnetron sputtering," Thin Solid Films 681, 15–22 (2019).
11. Ö. D. Coşkun and T. Zerrin, "Optical, structural and bonding properties of diamond-like amorphous carbon films deposited by DC magnetron sputtering," Diam. Relat. Mater. 56, 29–35 (2015).
12. L. R. Shaginyan, A. A. Onoprienko, V. F. Britun, and V. P. Smirnov, "Influence of different physical factors on microstructure and properties of magnetron sputtered amorphous carbon films," Thin Solid Films 397, 288–295 (2001).
13. D. Gibson and S. Song, "Apparatus and methods for depositing durable optical coatings," GB 2561865, (April 25, 2017).
14. N. H. Nickel, "Semiconductors and Semimetals," in Semiconductors and Semimetals, 1st Edition (Academic, 1991), Vol. 61, pp. 165–180.
15. VITRON Spezialwerkstoffe GmbH, "Infrared Chalcogenide Glass IG4," https://www.infrared-materials.com/upload/13623010-1219schott-ig4.pdf. (accessed 5th Nov 2019)
16. S. K. O. Leary, S. R. Johnson, and P. K. Lim, "The relationship between the distribution of electronic states and the optical absorption spectrum of an amorphous semiconductor : An empirical analysis The relationship between the distribution of electronic states and the optical absorption spectrum of," 3334, (2012).
17. R. Jacobsson, "Optical Properties of a Class of Inhomogeneous Thin Films," Opt. Acta Int. J. Opt. 10, 309–323 (1963).
18. C. Bédard and A. Destexhe, "Kramers-Kronig Relations and the Properties of Conductivity and Permittivity in Heterogeneous Media," J. Electromagn. Anal. Appl. 10, 34–51 (2018).
19. J. Hong, A. Goullet, and G. Turban, "Optical characterization of hydrogenated amorphous carbon (a-C:H) thin films deposited from methane plasma," Thin Solid Films 364, 144–149 (2000).
20. R. N. Tiwari, J. N. Tiwari, L. Chang, and M. Yoshimura, "Enhanced Nucleation and Growth of Diamond Film on Si by CVD Using a Chemical Precursor," J. Phys. Chem. C 115, 16063–16073 (2011).
21. A. R. Franco Jr., G. Pintaúde, A. Sinatora, C. E. Pinedo, and A. P. Tschiptschin, "The use of a vickers indenter in depth sensing indentation for measuring elastic modulus and vickers hardness," Mater. Res. 7, 483–491 (2004).
22. A. K., A. Varade, N. R. K., S. Dhan, C. M., B. N., and P. Krishna, "Synthesis of high hardness IR optical coating using diamond-like carbon by PECVD at room temperature," Diam. Relat. Mater. 78, 39–43 (2017).
23. G. G. Stoney, "The Tension of Metallic Films Deposited by Electrolysis," Proc. R. Soc. A Math. Phys. Eng. Sci. 82, 172–175 (1909).
24. MIL-C-48497A, Military Specification: Coating, Single or Multilayer, Interference: Durability Requirements (14 March 1997), http://everyspec.com/MIL-SPECS/MIL-SPECS-MIL-C/MIL-C-48497A_NOTICE-1_26219/ (accessed 5th Nov 2019)
25. H.A. Macleod, Thin Film Optical Filters, Institute of physics, London (2001)